Seminars in Cell and Developmental Biology 167 (2025) 1–9

Contents lists available at ScienceDirect

Seminars in Cell and Developmental Biology

journal homepage: www.elsevier.com/locate/semcdb

Review

Spatial omics shed light on the tumour organisation of glioblastoma

James R. Whittle [a,b,c], Jurgen Kriel [a,b], Oluwaseun E. Fatunla [a,b], Tianyao Lu [a], Joel J.D. Moffet [a,b], Montana Spiteri [a], Sarah A. Best [a,b,*,1], Saskia Freytag [a,b,*,1]

[a] Personalised Oncology Division, The Walter and Eliza Hall Institute of Medical Research, Melbourne, Australia
[b] Department of Medical Biology, University of Melbourne, Melbourne, Australia
[c] Department of Medical Oncology, Peter MacCallum Cancer Centre, Melbourne, Australia

ARTICLE INFO

Keywords:
Glioblastoma
Tumour microenvironment
Spatial omics
Spatial transcriptomics
Spatial metabolomics

ABSTRACT

The glioblastoma tumour microenvironment is characterised by immense heterogeneity, with malignant and non-malignant cells that interact in a complex ecosystem. Emerging evidence suggests that the tumour microenvironment is key in facilitating rapid proliferation, invasion, migration and cancer cell survival, crucial for treatment resistance. Spatial omics technologies have enabled the molecular characterisation of regions or individual cells within their spatial context, providing previously unattainable insights into the complex organisation of the glioblastoma tumour microenvironment. Understanding this organisation is crucial for the development of new therapeutics and novel diagnostic tools that guide patient care. This review explores spatial omics technologies and how they have contributed to the development of a model outlining the architecture of the glioblastoma tumour microenvironment.

1. Introduction

Glioblastoma (GBM) is the most aggressive primary brain tumour with dismal 5-year survival rates of less than 5 % [1]. Despite a rapidly expanding repertoire of novel biologics and immunotherapy in cancer care, GBM treatment for the past two decades has relied primarily on standard cytotoxic chemotherapy as the only systemic therapy with a proven survival benefit. The clinical stagnation of GBM treatment can be in part attributed to the heterogeneous nature of the tumour microenvironment (TME) [2], representing a complex ecosystem consisting of malignant cells, immune cells, vasculature, and other non-malignant cells. Due to its diverse and dynamic nature, the TME plays a crucial role in mediating complex phenomena, such as tumour progression and treatment response.

The rapid evolution of single cell RNA sequencing (scRNA-seq) has substantially broadened our understanding of the GBM TME [3]. Using scRNA-seq, *Neftel et al.* revealed four tumour cell states of GBM; neural progenitor cell-like (NPC-like), oligodendrocyte precursor cell-like (OPC-like), astrocyte-like (AC-like) and mesenchymal-like (MES-like) [4]. The first three tumour cell states exhibit transcriptional traits reminiscent of neuronal, oligodendrocytic and astrocytic cell lineages in the normal brain, respectively [4,5]. The MES-like state is marked by characteristics of cancer stem cells and has been associated with recurrence [6]. These cell states influence and are responsive to their cellular surroundings. Using scRNA-seq in combination with functional studies, macrophages were found to promote the transition of all tumour cells to a MES-like state [7], while NPC-like and OPC-like tumour cells receive synaptic input from neurons allowing them to adopt more aggressive invasion mechanisms [8]. However, scRNA-seq is unable to provide spatial context due to the destruction of the tissue to isolate cells, constraining insights into the TME ecosystem [9]. Analyses that retain the spatial context are thus required to gain a comprehensive understanding of this complex TME.

Techniques that allow the measurement of many molecules simultaneously in intact tissue, termed spatial omics, have emerged as an attractive option to retain information on cellular organisation and have already yielded diverse insights into the GBM TME. In this review, we provide an overview of the spatial omics technologies. We aim to describe how these different technologies have advanced our understanding of the GBM TME: interaction with the immune system, reliance on the vasculature, addiction to neuronal signalling and impact of metabolic reprogramming, together with our perspective on future applications of these technologies for diagnostic purposes.

* Correspondence to: The Walter and Eliza Hall Institute of Medical Research, Parkville, Victoria 3052, Australia.
E-mail addresses: best@wehi.edu.au (S.A. Best), freytag.s@wehi.edu.au (S. Freytag).
[1] Co-senior and Corresponding Authors

https://doi.org/10.1016/j.semcdb.2024.12.006
Received 27 June 2024; Received in revised form 23 October 2024; Accepted 30 December 2024
Available online 8 January 2025

2. Spatially-resolved omics methods unravel GBM architecture

The GBM TME consists of many components and their interactions. Spatial omics, in particular spatial transcriptomics and proteomics, have revealed that these components form highly organised structures.

2.1. The trade-offs of plexity and resolution in spatial transcriptomics

Approaches for spatial transcriptomics can be broadly classified based on detection via next generation sequencing (NGS) or imaging (Fig. 1, Table 1). NGS-based approaches encode positional information onto transcripts which are then read out by sequencing [10], whereas imaging-based approaches leverage fluorescently labelled probes that directly tag transcripts that are detected by high-resolution microscopy across multiple rounds of imaging [10]. NGS and imaging approaches vary in terms of robustness, area size, cost, sensitivity, throughput, resolution and ease of use. NGS-based technologies are capable of sequencing gene expression level across the whole transcriptome and isolating cell populations [11]. However, they are limited in their resolution as currently applied methods bin transcripts into regions that can contain multiple cells and thus cannot achieve single cell resolution [11]. Even recent advancements allowing for subcellular resolution cannot fully isolate single-cell profiles due to the requirement of binning, though these are yet to be applied to study GBM [12,13]. These methods of spatial profiling hinder cell-specific questions such as ligand receptor interactions, although broader predictive methods remain possible [14]. In comparison, imaging-based methods can currently profile more than 1000 genes but vary in the size of their capture region - and while targeted probes can be precisely located at subcellular resolution, panels are limited in size and customisability.

Both NGS- and imaging-based strategies encounter difficulties in the analysis of their generated data. Cell segmentation is an important component of imaging-based analyses, as this determines which transcripts are assigned to individual cells [25]. Alternatively, segmentation can be guided by distribution of transcripts themselves [26]. In the context of the GBM TME, the elongated or irregular morphologies of tumour and neural cell types requires sophisticated model training [27,28], which has not yet produced a streamlined pipeline for accurate segmentation [29,30]. Segmentation is of limited benefit to NGS-based strategies due to the coarser resolution, requiring deconvolution methods to estimate the composition of small regions [30]. However, these cannot compensate for the general lack of single cell resolution and thus spatial transcriptomics data from popular NGS-based methods may provide more limited insights into spatial organisation than data generated using imaging-based platforms. Contrastingly, background noise and limited panel size are current areas undergoing improvement for imaging-based platforms to enhance findings.

2.2. Antibodies as the key to spatial proteomics

Spatial proteomics can either be achieved via mass spectrometry imaging (MSI) or antibody-based approaches (Fig. 1). MSI, like Secondary Ion Mass Spectrometry (SIMS), ionizes tissue sections to analyse the released molecules with mass spectrometry, generating spatially resolved maps of various biomolecules [31,32]. While this allows an unbiased examination of tissue sections, the application of MSI in spatial proteomics is limited due to technical challenges that include low spatial resolution, inability to detect low-abundance proteins and imprecise quantification due to sample preparation [33]. Moreover, MSI produces complex data, which require advanced computational tools for the identification of proteins [34]. Hence, antibody-based approaches, which provide greater versatility and specificity, are the dominant technique in spatial proteomics. Traditional antibody-based approaches, like immunohistochemistry and proximity ligation assay, are limited to the measurement of 1–4 proteins [35]. Approaches harnessing multiplexing and/or indexing have increased the number of proteins detected simultaneously. These include multiplexed immunohistochemistry (mIHC) [36], multiplexed immunofluorescence (mIF) [37], and CO-Detection by indEXin (CODEX) [38]. Relying on the principles of mIF, CODEX is a multiplexed single-cell imaging technology that employs the use of antibodies. Antibodies are conjugated to barcodes comprised of unique oligonucleotide sequences, enabling the detection of over 60 antigens at single-cell level in one tissue sample [39]. CODEX overcomes the limitations experienced in mIF such as tissue distortion, antibody-antibody interactions and longer incubation times. This is largely achieved by the fast sequential barcode readout through rapid

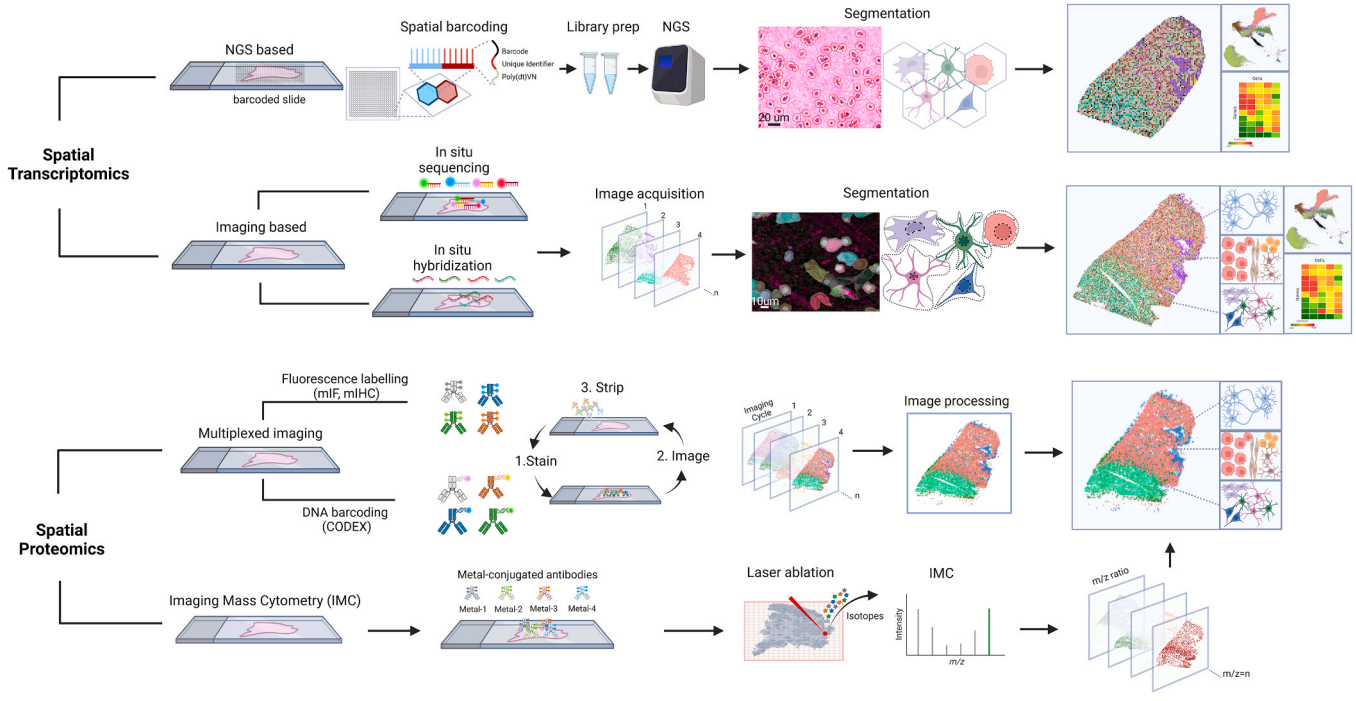

Fig. 1. Schematic representation of the workflows of spatial proteomics and transcriptomics methods used to profile the GBM TME.

Table 1
Spatial transcriptomics techniques available for use in the study of the GBM TME.

	Technology	Method	Resolution/Capture area	Targets	Ref.
NGS	LCM-seq	Laser capture microscopy (LCM)	Defined regions	mRNA Whole transcriptome	[15]
	Nanostring GeoMx	Digital spatial profiling (DSP) via photocleavable oligonucleotide barcodes	Defined regions, separated by marker expression	mRNA Whole Transcriptome	[16]
	10X Visium	Gene capture across an array of spots	55 μm spots with 100 μm distance between centers 6.5 × 6.5 mm capture region	mRNA Whole Transcriptome	[11]
	Slide-seq	Gene capture across an array of spots	10 μm spots	mRNA Whole Transcriptome	[17]
	10X Visium HD	Gene capture across an array of uniquely-barcoded oligonucleotide squares	Sub-cellular scale: 2 μm tiles binned into 8 × 8 μm regions 6.5 × 6.5 mm capture region	mRNA Whole Transcriptome	[13]
	STOmics Stereo-seq	DNA Nanoballs	Sub-cellular reolution: 0.2 μm spots with 0.5 μm distance between centers 13.2 × 13.2 mm capture region	mRNA Whole Transcriptome	[12]
Imaging - ISH	10X Xenium	Probe ligation, rolling circle amplification, and fluorophore hybridization Expansion segmentation or multimodal segmentation	Sub-cellular resolution 12 × 24 mm capture region	mRNA Up to 5000 genes	[18]
	EEL-FISH	RNA transfer via electrophoresis with expansion segmentation	Sub-cellular resolution 1 cm^2 capture region	mRNA 500 genes	[19]
	Nanostring CosMx	Fluorescent probe hybridisation with probabilistic cell-typing	Sub-cellular resolution 0.51 mm^2 capture region (up to 20/slide)	mRNA and proteins Up to 6000 genes 68 proteins	[20]
	MERSCOPE	error-robust barcodes	Sub-cellular resolution 3 cm^2 capture region	mRNA and proteins Up to 1000 genes 6 proteins	[21]
	RNAScope	Double Z probe design	Single-cell resolution 20 × 20 mm capture region	mRNA 12 genes	[22]
Imaging - ISS	HybISS	Padlock probes and rolling circle amplification with antibody-based segmentation	Sub-cellular resolution 60 mm^2 capture region	mRNA 200 genes	[23]
	STARmap	three-dimensional sequencing by ligation	Subcellular resolution	mRNA 1020 genes	[24]

binding and unbinding of fluorescent oligonucleotides [40]. The images generated are reconstructed to create a high-dimensional spatial map of the tissue, though imaging artifacts relating to corner bleaching have been documented [41]. Approaches exist that combine MSI and antibody-based methods to visualise the distribution of specific proteins in tissue sections, such as Imaging Mass Cytometry (IMC) [42], where antibodies conjugated to metal isotopes are quantified using a mass spectrometer.

2.3. Mapping the GBM architecture via spatial transcriptomics and proteomics

The application of spatial omics to patient GBM tissue samples cemented the notion of immense intra-tumoral heterogeneity [43]. While this had been apparent from previous studies using RNA-sequencing on multiple samples from the same tumour [44], spatial omics powerfully demonstrated the extent of this diversity and spatial intermixing, whereby proximal regions can be dominated by different tumour cell states [45] and clonal lineages [46]. As a result, many spatial omics technologies have been applied with the intent to learn about the tumour architecture and understand the principles guiding its organisation. In 2022, *Ravi et al.* were the first to systematically address this challenge by using spatial transcriptomics generated from 20 GBM tumours with the 10X Visium technology [47]. This dataset has since been used multiple times to help make new discoveries or validate findings on the organisation of GBM tumours (Supplementary Materials). These and other studies using spatial transcriptomics and proteomics have converged on the existence of four distinct niches in the GBM TME: the non-necrotic tumour core, hypoxia-associated mesenchymal neighbourhoods, perivascular niches rich in immune cells, and the invasive edge where tumour cells meet neurons (Fig. 2).

The non-necrotic tumour core makes up the bulk of the tumour and is densely packed with malignant cells [48]. Use of NGS-based spatial transcriptomic methods characterised these cells as predominately of the OPC-like tumour state [49,50]. However, application of newer spatial technologies with single cell resolution have refined this model by revealing considerable intermixing of AC-like and OPC-like states in the tumour core [45,51]. This heterogeneity may result from cellular interactions enabled by immune cell infiltration and increased cell density [52]. Indeed, an early study investigating immune cells in 47 tumour explants by CODEX found that the tumour core was rich in immunosuppressive macrophages and microglia cells [48]. More recently, the co-localisation of AC-like tumour cells and microglia cells in the core was confirmed across spatial transcriptomics data generated by CosMx, 10X Visium, and GeoMx [45]. Reanalysis of the *Ravi et al.* data shows that these microglia share decreased levels of homeostatic genes, co-expression of pro- and anti-inflammatory molecules, and increased levels of canonical markers with pro-tumoural macrophages [53]. Furthermore, spatial transcriptomics elucidated ligand-receptor pairs that govern the interaction of myeloid cells with tumour cells in GBM. Notable pairs include *VISTA-VSIG3* [54] and *ANXA1-FPR1* [55], which have been demonstrated to associate with poor survival or induce immunosuppressive environments, respectively. In BRAF mutated GBM tumours, spatial transcriptomics of tumour slices treated with a BRAF/MEK inhibitor further indicated a critical role of MAPK/ ERK signalling in modulating interactions between tumour and myeloid cells [56]. This result suggests the MAPK/ ERK pathway as a promising target to enhance immunotherapy.

GBM tumours present with tissue hypoxia that occurs in distinct

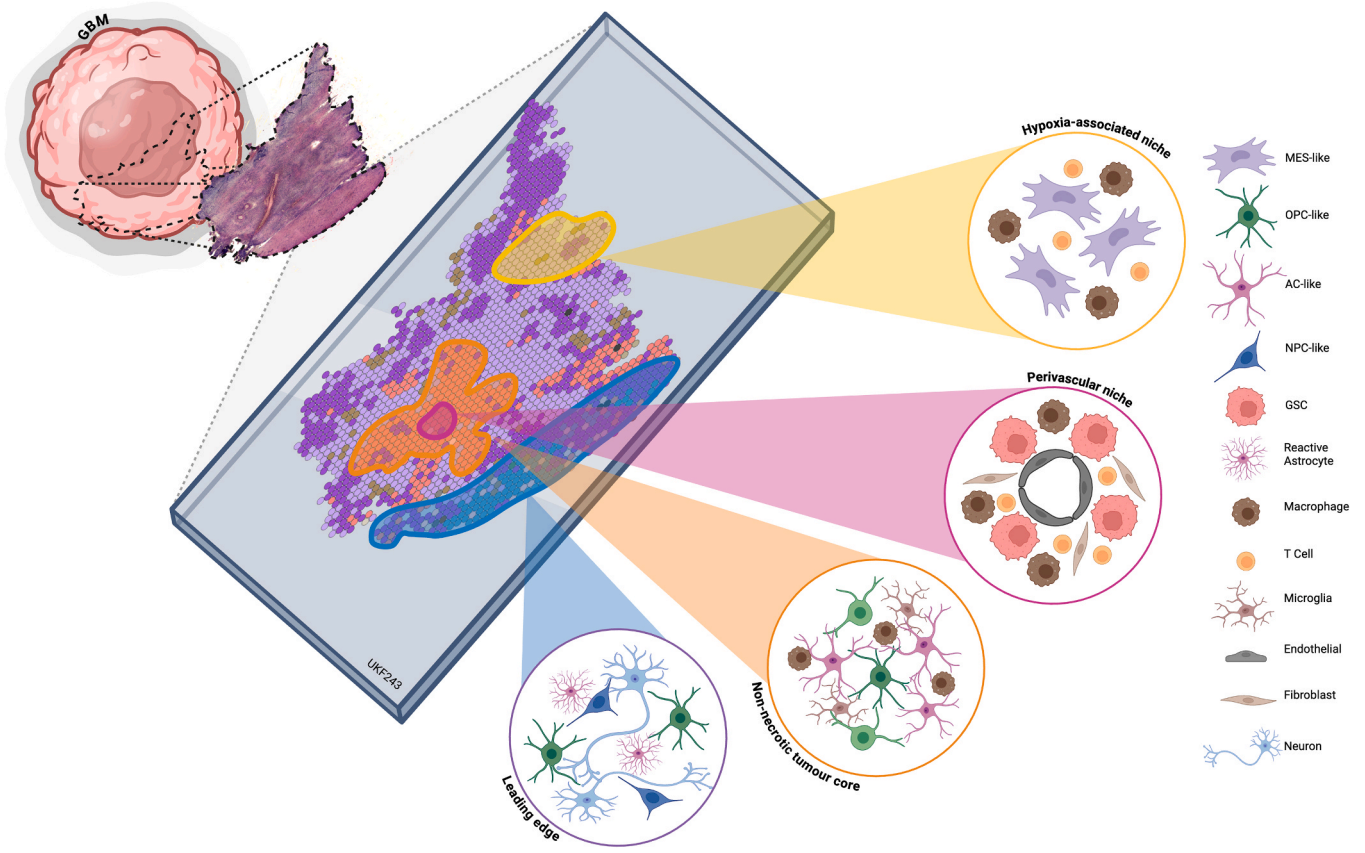

Fig. 2. Model of the architecture of GBM tumours based on spatial omics. The GBM TME is characterised by four regional niches; the leading edge, non-necrotic tumour core, perivascular niche, and hypoxia-associated niche. Each niche is populated by specific cell types that either perpetuate or result from the unique environmental conditions of the niche.

regions and is associated with extensive metabolic reprogramming [57]. These niches are critical as they increase the velocity of GBM evolution and are associated with poorer patient survival [58,59]. Spatial transcriptomics has revealed that hypoxic niches are preferentially populated by MES-like tumour cells, impair cell proliferation, and induce cell migration programs [55]. The hypoxic niche is associated with infiltrating immune cells, such as T cells, macrophages, and monocytes, which promote an immunosuppressive phenotype through the expression of cytokines and an increase in extracellular adenosine [55,60,61]. Activated myeloid cells surrounding the hypoxic niche produce creatine to support the growth of tumour cells [62], with macrophages infiltrating the niche as opposed to microglia [61]. Using 10X Visium data generated from genetically engineered mouse models of GBM, a subset of these macrophages in the hypoxic region has been shown to phagocytose myelin debris and transfer derived lipids to MES-like cells fuelling tumour growth [63]. The interactions between tumour and immune cells appear to be necessary for the generation of hypoxic zones. Importantly, the effect of hypoxia extends beyond the visibly necrotic areas and appears to be a driver of global spatial organisation of the tumour, with tumours impacted by hypoxia displaying more organisation than those tumours that lack hypoxia [51,64]. This effect on spatial organisation might be mediated by necrosis and aberrant vasculature, which are caused by oxidative stress. Moreover, spatial transcriptomic analysis on 55 GBM samples found that this architecture is reminiscent of a response in normal tissue to wound healing, which may implicate a functional program driving the development of this hypoxic niche [64].

The perivascular niche is thought to harbour pluripotent glioma stem cells that maintain self-renewal capacity through their interaction with the endothelium [65]. Intriguingly, this niche was found to be inhabited by cancer associated fibroblasts, which through secretion and remodelling of the extracellular matrix create a supportive environment for the maintenance and proliferation of glioma stem cells [66]. Beyond this, studies applying both spatial transcriptomics and/or proteomics have further characterised the perivascular niche as containing infiltrative immune cells, such as bone marrow derived macrophages, T and B cells [45,51,67,68]. The macrophages in the perivascular niche have been demonstrated to express signatures of phagocytosis and antigen-presentation [53]. Interestingly, use of single cell resolution spatial transcriptomics suggested that macrophages in this region may impair migration of abundant T cells high in *GZMK* expression, which are abundant in GBM, further into the tumour core [69]. While different studies conducted with spatial omics agree on co-localisation of immune and endothelial cells, they disagree on the dominant tumour cell state surrounding the vasculature in GBM. A study by *Greenwald et al.* found that predominately tumour cells in the OPC-like state co-locate with endothelial cells [51]. This observation is consistent with findings from an independent study using 10X Visium on 3 patient samples [70] and a study using HyBiSS with 199 probes on 2 patient samples [71]. In contrast, spatial transcriptomics data generated using EEL-FISH of 57 sections from 27 patients found that AC-like tumour cells, rich in *CRYAB* expression, co-locate with endothelial cells. EEL-FISH, unlike 10X Visium, provides single cell resolution but has poor sensitivity. With the limitations in study size and technologies, future studies using spatial omics are needed to fully characterise the microenvironment around the vasculature.

Recently, synaptic connections between healthy neurons and adjacent malignant glioma cells have been discovered at the leading edge. These neuron-glioma synapses have been observed in xenograft models and resected patient samples, with NPC- or OPC-like states integrating into surrounding neuronal circuitry and communicating through

synaptic architecture [8]. The communication is mediated by mechanisms including AMPA receptors and paracrine signalling via *NLGN3* and *BDNF* [72,73]. Neuron-glioma synapses increase branching of tumour microtubules, and drive glioma invasion and growth by co-opting migration strategies reminiscent of neuronal progenitor cells [8,74]. Signalling between neurons and glioma is also bidirectional, with neuronal excitability increased via glutamate secretion from glioma cells [75]. While pioneering immuno-electron microscopy and single cell sequencing demonstrated this neuron-glioma interface, spatial technologies promise to further characterise how this connectivity aids tumorigenesis. A study employing 10X Visium demonstrated associations of neurons with reactive astrocytes and NPC-like tumour states [76]. Consistent with the spatial heterogeneity of GBM samples, individual samples displayed a continuum of neural signature strength enriched for synaptic characteristics that transitioned across space, with malignant and neuroglial states enriched in high neural areas [76].

3. Metabolic niches

Spatial metabolomics and lipidomics of GBM samples, both primary patient tissue and murine models, has unveiled a new dimension of niches, which was unable to be parsed in bulk samples.

3.1. Spatial metabolomics technologies

The most popular spatial metabolomics technologies rely on MSI, which involves the desorption and ionisation of analytes and their accelerated within an electrical field towards a mass analyser. There are three types of ionisation methods, matrix-assisted laser desorption/ionisation (MALDI) [77], desorption electrospray ionisation (DESI) [78], and SIMS, which is also commonly utilised for proteins (Table 2).

MALDI-MSI combines a high energy laser beam with energy absorbing matrix molecules. Matrix is sprayed onto the tissue and forms crystalline structures with the analytes after dehydration. When exposed to the laser, the matrix absorbs the energy and assists in the release of analytes that can then be detected in a mass analyser [77]. The choice of matrices significantly determines the range of molecules that can be identified and at what sensitivity. Recently, a study investigating different matrices for studying brain cancer reported that the use α-cyano-4-hydroxycinnamic acid matrix with positive polarity offered the best performance of 5 different matrices for small molecules (70–400 m/z) and small lipids (400–1000 m/z) [79]. Unlike the laser used in MALDI-MSI, DESI-MSI uses electrically charged droplets to ionise analytes. To form and apply these droplets, DESI-MSI utilises a high-voltage electric field applied to a solvent. Upon contact between the droplets and the analytes, the charged droplets propel the analytes towards a mass analyser where they can be detected. Typical solvent used in electrospray is volatile and polar, including water, methanol, acetonitrile, and their mixtures. Like MALDI-MSI, the choice of solvent critically impacts the detection of the range of analytes [80].

Unlike ionisation-based MSI methods, Raman spectroscopy is a non-invasive and label-free optical tool that allows the detection of metabolites across tissue [81]. Instead of identifying the molecules by their mass, Raman spectroscopy exploits that light is inelastically scattered from a sample when it is illuminated by light from a laser. The energy of the scattered photons is different from that of the incident photons producing the Raman spectrum which serves as a fingerprint for the composition and structure of the irradiated area. Newer fast atom bombardment methods, like stimulated Raman spectroscopy utilising high-frequency phase-sensitive detection allow a resolution of ~450 nm comparable to fluorescence microscopy, greater sensitivity, faster imaging speeds, background-free and readily interpretable chemical contrast compared to traditional spontaneous Raman spectroscopy [82]. Hence, Raman spectroscopy has been popular for real-time imaging and diagnostic purposes (discussed below).

Table 2
MSI-based spatial metabolomics techniques utilised in the study of the GBM TME.

	MALDI-MSI	DESI-MSI	SIMS
Ionisation method	Laser desorption/ionisation	Electrospray desorption/ionisation	Focused ion beams
Working environment	High vacuum/Ultra-high vacuum/Atmospheric pressure	Ambient	Low vacuum (Wet SIMS)/High vacuum/Ultra-high vacuum
Spatial resolution	10 μm - 150 μm	40 μm - 400 μm	10 nm – 50 nm
Commonly used mass spectrometry analysers	– Time of flight (ToF) – Quadrupole Ion Trap (QIT) – Orbitrap – Fourier Transform Ion Cyclotron Resonance (FT-ICR)	– ToF – QIT – Orbitrap – FT-ICR	– ToF – Magnetic Sector – QIT

3.2. Metabolic diversity in GBM

Spatial metabolomics has yielded distinct metabolic activity that distinguish tumour and normal brain. Such metabolites include the polyamine spermidine, which has been found in MALDI-MSI spatial studies in transplanted murine tumours (CT-2A and GL-261 models) to be significantly enriched in tumour compared to normal brain [83]. Importantly, spermidine abundance impacts on the activity of tumour infiltrating CD8 T cells [83] and tumour associated myeloid cells [84], with polyamine inhibitors enhancing survival in immunocompetent mice. Purines have also been found to play an important role in the TME, with MALDI-MSI analysis of patient GBM tumours finding that purine metabolism is among the most significantly enriched metabolic pathways [60]. Moreover, adenosine was found to correlate to the protein expression of CD73, which interacts with microglial CD39 protein, with spatial proximity predictive of poor outcomes for adult GBM and paediatric diffuse midline glioma patients [60], further supporting the importance of spatial analyses of the TME.

Tumour intrinsic niches have also been identified by spatial lipidomic profiling, with the abundance and class of lipids differing between tumour regions and predictive of the subtype of glioma. In a study of 36 patients with gliomas of different histological grades [85], a machine learning classifier was built to determine the subtype of glioma based on the DESI-MSI spatial lipidomic input data. Qualitative sampling of glycerophosphoinositols, glycerophosphoserine and sulfatide lipid species, in addition to specific peaks including arachidonic acid (m/z 303.2), was used in the classifier to determine glioma subtype [85]. This suggests that different subtypes of glioma share intrinsic lipid metabolic profiles and may metabolise drugs differently. Furthermore, analysis of GBM xenograft murine models using MALDI-MSI identified that long-chain acylcarnitines were detected with increased intensity at the tumour edge compared to the core [86]. Together, these studies find that the differing mechanisms of fatty acid metabolism may influence drug distribution due to differing affinity and transport mechanisms both throughout the tumour and between different subtypes of glioma in patients.

A clinically utilised metabolic pathway in GBM is the hydrolysis of 5-aminolevulinic acid (5-ALA) to protoporphyrin IX (PpIX). PpIX is fluorescent under blue light, and this pathway is harnessed in fluorescence guided neurosurgery, where the pro-drug Gliolan® (5-ALA) is administered to patients prior to surgery to fluorescently demarcate infiltrative tumours outside the magnetic resonance imaging (MRI) contrast-enhanced regions of GBM [87]. Combining 5-ALA positive spatial regions with transcriptomics has enabled the description of gene

signatures associated with aggressive tumours and proteomic analysis revealing pro-survival signatures [88]. Importantly, defining discrete metabolic regions using real-time fluorescence allows for the intra-operative distinction of the peri-necrotic zone, bulk tumour, and tumour margin regions [88], whereby effective removal of 5-ALA positive regions was found to effectively identify the immune reactive zone beyond the tumour core [88]. Thus, real-time spatial intraoperative analysis of distinct metabolic pathways could leverage the intrinsic phenotype of the GBM cells (discussed below).

Spatial metabolomics has additionally played a role in better understanding GBM subtypes. The hydrolysis of 5-ALA to PpIX in tumour cells was found to associate with a MES-like phenotype (wound response/glycolytic signature), which was distinct from the tumour cells at the core, using transcriptomics of spatially defined 5-ALA metabolising regions [89]. The most striking association with the MES-like tumour cells is with the hypoxic niche in GBM, where loss of oxygen and metabolic deterioration leads to genomic instability [90]. Using MALDI-MSI of 6 GBM samples, regions of hypoxia were detected, in-line with their transcriptionally proposed locations, with strong enrichment for glycolysis and amino sugar metabolism [47]. Such glycolysis can result in an acidified TME, which can be harnessed to facilitate tumour invasion and the release of purine metabolites, which impact immune interactions [47,60,91].

4. Spatial omics is set to change GBM diagnosis and treatment

Currently, specific measures of cellular composition, microanatomical location and associated tissue interactions do not enter the appraisal of pathological assessment in clinical routine. Thus, the next frontier for spatial omics will be the integration into clinical practice. A deeper understanding of cell states and spatial architecture, such as the identification of spatial biomarkers of response could inform diagnosis, prognosis, and guide treatment selection. For this to be effective, studies will need to consider the cost, available expertise, and timeliness of results to inform clinical care. To overcome these limitations, one approach is to leverage deep learning approaches that utilises available spatial transcriptomic data to train a model that can then predict outcomes from widely available histology images. The requirement for such an approach necessitates that gene expression can be inferred from cell morphology. From a cohort of 23 GBM samples with matched spatial transcriptomics and histology images, *Zheng et al.* developed a convolutional neural network and applied this to 410 patients with histology sections [49]. This model could accurately predict the regional composition in terms of tumour cell states and immune cell types. Notably, spatial interactions between tumour cell states could predict survival; for example, increased connectivity between AC-like cell states decreases survival, compared to patients with TMEs where AC-like cell states connect with other cell states, highlighting the capacity of spatial omics data to improve prognostication.

Further efforts are required to bring spatial omics technologies into real-time utility to inform neurosurgical decision making. While frozen sections taken at the time of surgery have long been part of routine clinical practice with reported high diagnostic accuracy [92], they are time and labour intensive [93], and have limited influence on extent of resection. Therefore, there is a need for technology, such as Raman spectroscopy [94,95] and DESI-MSI [96], that can deliver more rapid results intraoperatively facilitating a more comprehensive guide on heterogenous tumour margins and residual disease at the resection cavity. Raman spectroscopy has been used to discriminate tumour margins, which can be used to actively guide neurosurgery, and distinguish between GBM and *IDH*-mutant glioma, thus actively guide neurosurgery [94]. Other approaches use non-spatial techniques, such as methylation arrays, in combination with artificial intelligence algorithms trained on matched spatial omics data to guide clinical decision making. For example, using such an algorithm trained on methylation signatures, *Drexler et al.* distinguishes between high-neural signatures in GBM patients who may benefit from more aggressive surgical resection [76]. This result illustrates that real-time molecular measurements may in the future guide neurosurgeons to maximise the risk-benefit equation during surgical procedures and could permit rapid enrolment in clinical trials, ultimately changing clinical practice.

5. Conclusions

Rapidly evolving spatial omics technologies have already provided a model of the organisation of the GBM TME. This model suggests that targeted treatments aimed at exploiting specific niches, such as hypoxia-associated neighbourhoods, are required. While there are some early therapeutic targets and improved understanding of disease mechanism, expanding beyond spatial and into the temporal dimension will be key to drive further discoveries and understand cell dynamics impacting tumourigenesis and immune regulation. Perioperative clinical trials utilising spatial transcriptomics longitudinally hold promise to investigate cell dynamics in patients [97]. Beyond their impact on drug discovery for GBM, spatial omics will revolutionise the diagnosis and prognostication of GBM either via their direct application or more likely using models trained on spatial omics or multi-omics data, once more readily available. This will ultimately pave the way for accelerated tumour diagnosis and personalised treatment for patients.

Competing interest

SF reports a relationship with NanoString Technologies Inc that includes: travel reimbursement. SAB reports a relationship with NanoString Technologies Inc that includes: funding grants. All other authors declare that they have no competing interests. All authors have contributed to and approved the content of the manuscript and its submission to Seminars in Cell and Developmental Biology. Any affiliations or collaborations are as stated in the manuscript.

Funding

This work was made possible and financially supported in part through the authors' membership of the Brain Cancer Centre, support from Carrie's Beanies 4 Brain Cancer, a Venture Grants Scheme administered by Cancer Council Victoria (VG2022 to SAB, SF, JRW) and through Victorian State Government Operational Infrastructure Support and Australian Government NHMRC Independent Research Institutes Infrastructure Support Scheme (IRIISS). Support from the Victorian Cancer Agency Mid-Career Research Fellowship (MCRF22003 to SAB), WEHI Johnson PhD Scholarship and an Australian Government Research Training Program (RTP) Scholarship (JJDM), CSL Translational Data Science Scholarship (JJDM), WEHI IPSI Scholarship (OEF), Melbourne Research Scholarship (OEF) and Gregg Symons Scholarship for Brain Cancer Research (OEF).

Supplementary materials

Table: Studies using spatially resolved data to investigate the GBM TME.

Appendix A. Supporting information

Supplementary data associated with this article can be found in the online version at doi:10.1016/j.semcdb.2024.12.006.

References

[1] P.D. Delgado-López, E.M. Corrales-García, Survival in glioblastoma: a review on the impact of treatment modalities, Clin. Transl. Oncol. 18 (2016) 1062–1071.
[2] M.I. De Silva, B.W. Stringer, C. Bardy, Neuronal and tumourigenic boundaries of glioblastoma plasticity, Trends Cancer 9 (2023) 223–236.

[3] Y.A. Yabo, D.H. Heiland, Understanding glioblastoma at the single-cell level: recent advances and future challenges, PLoS Biol. 22 (2024) e3002640.
[4] C.P. Couturier, S. Ayyadhury, P.U. Le, J. Nadaf, J. Monlong, G. Riva, R. Allache, S. Baig, X. Yan, M. Bourgey, C. Lee, Y.C.D. Wang, V. Wee Yong, M.-C. Guiot, H. Najafabadi, B. Misic, J. Antel, G. Bourque, J. Ragoussis, K. Petrecca, Single-cell RNA-seq reveals that glioblastoma recapitulates a normal neurodevelopmental hierarchy, Nat. Commun. 11 (2020), https://doi.org/10.1038/s41467-020-17186-5.
[5] C. Neftel, J. Laffy, M.G. Filbin, T. Hara, M.E. Shore, G.J. Rahme, A.R. Richman, D. Silverbush, M.L. Shaw, C.M. Hebert, J. Dewitt, S. Gritsch, E.M. Perez, L. N. Gonzalez Castro, X. Lan, N. Druck, C. Rodman, D. Dionne, A. Kaplan, M. S. Bertalan, J. Small, K. Pelton, S. Becker, D. Bonal, Q.-D. Nguyen, R.L. Servis, J. M. Fung, R. Mylvaganam, L. Mayr, J. Gojo, C. Haberler, R. Geyeregger, T. Czech, I. Slavc, B.V. Nahed, W.T. Curry, B.S. Carter, H. Wakimoto, P.K. Brastianos, T. T. Batchelor, A. Stemmer-Rachamimov, M. Martinez-Lage, M.P. Frosch, I. Stamenkovic, N. Riggi, E. Rheinbay, M. Monje, O. Rozenblatt-Rosen, D.P. Cahill, A.P. Patel, T. Hunter, I.M. Verma, K.L. Ligon, D.N. Louis, A. Regev, B.E. Bernstein, I. Tirosh, M.L. Suvà, An integrative model of cellular states, plasticity, and genetics for glioblastoma, Cell 178 (2019) 835–849.e21.
[6] F.S. Varn, K.C. Johnson, J. Martinek, J.T. Huse, M.P. Nasrallah, P. Wesseling, L.A. D. Cooper, T.M. Malta, T.E. Wade, T.S. Sabedot, D. Brat, P.V. Gould, A. Wöehrer, K. Aldape, A. Ismail, S.K. Sivajothi, F.P. Barthel, H. Kim, E. Kocakavuk, N. Ahmed, K. White, I. Datta, H.-E. Moon, S. Pollock, C. Goldfarb, G.-H. Lee, L. Garofano, K. J. Anderson, D. Nehar-Belaid, J.S. Barnholtz-Sloan, S. Bakas, A.T. Byrne, F. D'Angelo, H.K. Gan, M. Khasraw, S. Migliozzi, D.R. Ormond, S.H. Paek, E.G. Van Meir, A.M.E. Walenkamp, C. Watts, T. Weiss, M. Weller, K. Palucka, L.F. Stead, L. M. Poisson, H. Noushmehr, A. Iavarone, R.G.W. Verhaak, GLASS Consortium, Glioma progression is shaped by genetic evolution and microenvironment interactions, Cell 185 (2022) 2184–2199.e16.
[7] T. Hara, R. Chanoch-Myers, N.D. Mathewson, C. Myskiw, L. Atta, L. Bussema, S. W. Eichhorn, A.C. Greenwald, G.S. Kinker, C. Rodman, L.N. Gonzalez Castro, H. Wakimoto, O. Rozenblatt-Rosen, X. Zhuang, J. Fan, T. Hunter, I.M. Verma, K. W. Wucherpfennig, A. Regev, M.L. Suvà, I. Tirosh, Interactions between cancer cells and immune cells drive transitions to mesenchymal-like states in glioblastoma, Cancer Cell 39 (2021) 779–792.e11.
[8] V. Venkataramani, Y. Yang, M.C. Schubert, E. Reyhan, S.K. Tetzlaff, N. Wißmann, M. Botz, S.J. Soyka, C.A. Beretta, R.L. Pramatarov, L. Fankhauser, L. Garofano, A. Freudenberg, J. Wagner, D.I. Tanev, M. Ratliff, R. Xie, T. Kessler, D. C. Hoffmann, L. Hai, Y. Dörflinger, S. Hoppe, Y.A. Yabo, A. Golebiewska, S. P. Niclou, F. Sahm, A. Lasorella, M. Slowik, L. Döring, A. Iavarone, W. Wick, T. Kuner, F. Winkler, Glioblastoma hijacks neuronal mechanisms for brain invasion, Cell 185 (2022) 2899–2917.e31.
[9] M. Piwecka, N. Rajewsky, A. Rybak-Wolf, Single-cell and spatial transcriptomics: deciphering brain complexity in health and disease, Nat. Rev. Neurol. 19 (2023) 346–362.
[10] Y. Fangma, M. Liu, J. Liao, Z. Chen, Y. Zheng, Dissecting the brain with spatially resolved multi-omics, J. Pharm. Anal. 13 (2023) 694–710.
[11] P.L. Ståhl, F. Salmén, S. Vickovic, A. Lundmark, J.F. Navarro, J. Magnusson, S. Giacomello, M. Asp, J.O. Westholm, M. Huss, A. Mollbrink, S. Linnarsson, S. Codeluppi, Å. Borg, F. Pontén, P.I. Costea, P. Sahlén, J. Mulder, O. Bergmann, J. Lundeberg, J. Frisén, Visualization and analysis of gene expression in tissue sections by spatial transcriptomics, Science 353 (2016) 78–82.
[12] A. Chen, S. Liao, M. Cheng, K. Ma, L. Wu, Y. Lai, X. Qiu, J. Yang, J. Xu, S. Hao, X. Wang, H. Lu, X. Chen, X. Liu, X. Huang, Z. Li, Y. Hong, Y. Jiang, J. Peng, S. Liu, M. Shen, C. Liu, Q. Li, Y. Yuan, X. Wei, H. Zheng, W. Feng, Z. Wang, Y. Liu, Z. Wang, Y. Yang, H. Xiang, L. Han, B. Qin, P. Guo, G. Lai, P. Muñoz-Cánoves, P. H. Maxwell, J.P. Thiery, Q.-F. Wu, F. Zhao, B. Chen, M. Li, X. Dai, S. Wang, H. Kuang, J. Hui, L. Wang, J.-F. Fei, O. Wang, X. Wei, H. Lu, B. Wang, S. Liu, Y. Gu, M. Ni, W. Zhang, F. Mu, Y. Yin, H. Yang, M. Lisby, R.J. Cornall, J. Mulder, M. Uhlén, M.A. Esteban, Y. Li, L. Liu, X. Xu, J. Wang, Spatiotemporal transcriptomic atlas of mouse organogenesis using DNA nanoball-patterned arrays, Cell 185 (2022) 1777–1792.e21.
[13] M.F. Oliveira, J.P. Romero, M. Chung, S. Williams, A.D. Gottscho, A. Gupta, S. E. Pilipauskas, S. Mohabbat, N. Raman, D. Sukovich, D. Patterson, S.E.B. Taylor, Visium HD Development Team, Characterization of immune cell populations in the tumor microenvironment of colorectal cancer using high definition spatial profiling, BioRxiv (2024), https://doi.org/10.1101/2024.06.04.597233.
[14] D. Pham, X. Tan, B. Balderson, J. Xu, L.F. Grice, S. Yoon, E.F. Willis, M. Tran, P. Y. Lam, A. Raghubar, P. Kalita-de Croft, S. Lakhani, J. Vukovic, M.J. Ruitenberg, Q. H. Nguyen, Robust mapping of spatiotemporal trajectories and cell-cell interactions in healthy and diseased tissues, Nat. Commun. 14 (2023) 7739.
[15] S. Nichterwitz, J.A. Benitez, R. Hoogstraaten, Q. Deng, E. Hedlund, LCM-seq: A method for spatial transcriptomic profiling using laser capture microdissection coupled with PolyA-based RNA sequencing. in: Methods in Molecular Biology, Springer New York, New York, NY, 2018, pp. 95–110.
[16] M.I. Toki, C.R. Merritt, P.F. Wong, J.W. Smithy, H.M. Kluger, K.N. Syrigos, G. T. Ong, S.E. Warren, J.M. Beechem, D.L. Rimm, High-plex predictive marker discovery for melanoma immunotherapy–treated patients using digital spatial profiling, Clin. Cancer Res. 25 (2019) 5503–5512.
[17] S.G. Rodriques, R.R. Stickels, A. Goeva, C.A. Martin, E. Murray, C.R. Vanderburg, J. Welch, L.M. Chen, F. Chen, E.Z. Macosko, Slide-seq: a scalable technology for measuring genome-wide expression at high spatial resolution, Science 363 (2019) 1463–1467.
[18] J.H. Lee, E.R. Daugharthy, J. Scheiman, R. Kalhor, T.C. Ferrante, R. Terry, B. M. Turczyk, J.L. Yang, H.S. Lee, J. Aach, K. Zhang, G.M. Church, Fluorescent in situ sequencing (FISSEQ) of RNA for gene expression profiling in intact cells and tissues, Nat. Protoc. 10 (2015) 442–458.
[19] L.E. Borm, A. Mossi Albiach, C.C.A. Mannens, J. Janusauskas, C. Özgün, D. Fernández-García, R. Hodge, F. Castillo, C.R.H. Hedin, E.J. Villablanca, P. Uhlén, E.S. Lein, S. Codeluppi, S. Linnarsson, Scalable in situ single-cell profiling by electrophoretic capture of mRNA using EEL FISH, Nat. Biotechnol. (2022), https://doi.org/10.1038/s41587-022-01455-3.
[20] D. Gyllborg, C.M. Langseth, X. Qian, E. Choi, S.M. Salas, M.M. Hilscher, E.S. Lein, M. Nilsson, Hybridization-based *in situ* sequencing (HybISS) for spatially resolved transcriptomics in human and mouse brain tissue, Nucleic Acids Res. 48 (2020) e112.
[21] K.H. Chen, A.N. Boettiger, J.R. Moffitt, S. Wang, X. Zhuang, RNA imaging. Spatially resolved, highly multiplexed RNA profiling in single cells, Science 348 (2015) aaa6090.
[22] F. Wang, J. Flanagan, N. Su, L.-C. Wang, S. Bui, A. Nielson, X. Wu, H.-T. Vo, X.-J. Ma, Y. Luo, RNAscope: a novel in situ RNA analysis platform for formalin-fixed, paraffin-embedded tissues, J. Mol. Diagn. 14 (2012) 22–29.
[23] S. He, R. Bhatt, C. Brown, E.A. Brown, D.L. Buhr, K. Chantranuvatana, P. Danaher, D. Dunaway, R.G. Garrison, G. Geiss, Others, High-plex imaging of RNA and proteins at subcellular resolution in fixed tissue by spatial molecular imaging, Nat. Biotechnol. 40 (2022) 1794–1806.
[24] X. Wang, W.E. Allen, M.A. Wright, E.L. Sylwestrak, N. Samusik, S. Vesuna, K. Evans, C. Liu, C. Ramakrishnan, J. Liu, G.P. Nolan, F.-A. Bava, K. Deisseroth, Three-dimensional intact-tissue sequencing of single-cell transcriptional states, Science 361 (2018) eaat5691.
[25] M. Pachitariu, C. Stringer, Cellpose 2.0: how to train your own model, Nat. Methods 19 (2022) 1634–1641.
[26] V. Petukhov, R.J. Xu, R.A. Soldatov, P. Cadinu, K. Khodosevich, J.R. Moffitt, P. V. Kharchenko, Cell segmentation in imaging-based spatial transcriptomics, Nat. Biotechnol. 40 (2022) 345–354.
[27] X. Fu, Y. Lin, D.M. Lin, D. Mechtersheimer, C. Wang, F. Ameen, S. Ghazanfar, E. Patrick, J. Kim, J.Y.H. Yang, BIDCell: biologically-informed self-supervised learning for segmentation of subcellular spatial transcriptomics data, Nat. Commun. 15 (2024), https://doi.org/10.1038/s41467-023-44560-w.
[28] J. Kriel, J.J.D. Moffet, T. Lu, O.E. Fatunla, V.K. Narayana, A. Valkovic, A. Maluenda, M.J. McConville, E. Tsui, J.R. Whittle, S.A. Best, S. Freytag, An integrative spatial multi-omic workflow for unified analysis of tumor tissue, BioRxiv (2024), https://doi.org/10.1101/2024.10.15.618574.
[29] R. Li, M. Zhu, J. Li, M.S. Bienkowski, N.N. Foster, H. Xu, T. Ard, I. Bowman, C. Zhou, M.B. Veldman, X.W. Yang, H. Hintiryan, J. Zhang, H.-W. Dong, Precise segmentation of densely interweaving neuron clusters using G-Cut, Nat. Commun. 10 (2019), https://doi.org/10.1038/s41467-019-09515-0.
[30] S. Fang, B. Chen, Y. Zhang, H. Sun, L. Liu, S. Liu, Y. Li, X. Xu, Computational approaches and challenges in spatial transcriptomics, Genom. Proteom. Bioinforma. 21 (2023) 24–47.
[31] A.M. Belu, D.J. Graham, D.G. Castner, Time-of-flight secondary ion mass spectrometry: techniques and applications for the characterization of biomaterial surfaces, Biomaterials 24 (2003) 3635–3653.
[32] K. Chughtai, R.M.A. Heeren, Mass spectrometric imaging for biomedical tissue analysis, Chem. Rev. 110 (2010) 3237–3277.
[33] B. Shruthi, P. Vinodhkumar, Selvamani, Proteomics: a new perspective for cancer, Adv. Biomed. Res. 5 (2016) 67.
[34] A.G. Birhanu, Mass spectrometry-based proteomics as an emerging tool in clinical laboratories, Clin. Proteom. 20 (2023), https://doi.org/10.1186/s12014-023-09424-x.
[35] W.C.C. Tan, S.N. Nerurkar, H.Y. Cai, H.H.M. Ng, D. Wu, Y.T.F. Wee, J.C.T. Lim, J. Yeong, T.K.H. Lim, Overview of multiplex immunohistochemistry/immunofluorescence techniques in the era of cancer immunotherapy, Cancer Commun. 40 (2020) 135–153.
[36] M.R. Dandrea, P.A. Reiser, N.A. Gumula, B.M. Hertzog, P. Andrade-Gordon, Application of triple immunohistochemistry to characterize amyloid plaque-associated inflammation in brains with Alzheimer's disease, Biotech. Histochem. 76 (2001) 97–106.
[37] C.-W. Peng, X.-L. Liu, C. Chen, X. Liu, X.-Q. Yang, D.-W. Pang, X.-B. Zhu, Y. Li, Patterns of cancer invasion revealed by QDs-based quantitative multiplexed imaging of tumor microenvironment, Biomaterials 32 (2011) 2907–2917.
[38] S. Black, D. Phillips, J.W. Hickey, J. Kennedy-Darling, V.G. Venkataraaman, N. Samusik, Y. Goltsev, C.M. Schürch, G.P. Nolan, CODEX multiplexed tissue imaging with DNA-conjugated antibodies, Nat. Protoc. 16 (2021) 3802–3835.
[39] Y. Goltsev, N. Samusik, J. Kennedy-Darling, S. Bhate, M. Hale, G. Vazquez, S. Black, G.P. Nolan, Deep profiling of mouse splenic architecture with CODEX multiplexed imaging, Cell 174 (2018) 968–981.e15.
[40] J.W. Hickey, E.K. Neumann, A.J. Radtke, J.M. Camarillo, R.T. Beuschel, A. Albanese, E. McDonough, J. Hatler, A.E. Wiblin, J. Fisher, J. Croteau, E.C. Small, A. Sood, R.M. Caprioli, R.M. Angelo, G.P. Nolan, K. Chung, S.M. Hewitt, R. N. Germain, J.M. Spraggins, E. Lundberg, M.P. Snyder, N.L. Kelleher, S.K. Saka, Spatial mapping of protein composition and tissue organization: a primer for multiplexed antibody-based imaging, Nat. Methods 19 (2022) 284–295.
[41] E.K. Neumann, N.H. Patterson, E.S. Rivera, J.L. Allen, M. Brewer, M. P. deCaestecker, R.M. Caprioli, A.B. Fogo, J.M. Spraggins, Highly multiplexed immunofluorescence of the human kidney using co-detection by indexing, Kidney Int 101 (2022) 137–143.
[42] C. Giesen, H.A.O. Wang, D. Schapiro, N. Zivanovic, A. Jacobs, B. Hattendorf, P. J. Schüffler, D. Grolimund, J.M. Buhmann, S. Brandt, Z. Varga, P.J. Wild, D. Günther, B. Bodenmiller, Highly multiplexed imaging of tumor tissues with subcellular resolution by mass cytometry, Nat. Methods 11 (2014) 417–422.

[43] M.E. Berens, A. Sood, J.S. Barnholtz-Sloan, J.F. Graf, S. Cho, S. Kim, J. Kiefer, S. A. Byron, R.F. Halperin, S. Nasser, J. Adkins, L. Cuyugan, K. Devine, Q. Ostrom, M. Couce, L. Wolansky, E. McDonough, S. Schyberg, S. Dinn, A.E. Sloan, M. Prados, J.J. Phillips, S.J. Nelson, W.S. Liang, Y. Al-Kofahi, M. Rusu, M.I. Zavodszky, F. Ginty, Multiscale, multimodal analysis of tumor heterogeneity in IDH1 mutant vs wild-type diffuse gliomas, PLoS One 14 (2019) e0219724.

[44] A. Sottoriva, I. Spiteri, S.G.M. Piccirillo, A. Touloumis, V.P. Collins, J.C. Marioni, C. Curtis, C. Watts, S. Tavaré, Intratumor heterogeneity in human glioblastoma reflects cancer evolutionary dynamics, Proc. Natl. Acad. Sci. 110 (2013) 4009–4014.

[45] J.J.D. Moffet, O.E. Fatunla, L. Freytag, J. Kriel, J.J. Jones, S.J. Roberts-Thomson, A. Pavenko, D.K. Scoville, L. Zhang, Y. Liang, A.P. Morokoff, J.R. Whittle, S. Freytag, S.A. Best, Spatial architecture of high-grade glioma reveals tumor heterogeneity within distinct domains, Neurooncol. Adv. 5 (2023), https://doi.org/10.1093/noajnl/vdad142.

[46] K.A. Walentynowicz, D. Engelhardt, S. Cristea, S. Yadav, U. Onubogu, R. Salatino, M. Maerken, C. Vincentelli, A. Jhaveri, J. Geisberg, T.O. McDonald, F. Michor, M. Janiszewska, Single-cell heterogeneity of EGFR and CDK4 co-amplification is linked to immune infiltration in glioblastoma, Cell Rep. 42 (2023) 112235.

[47] V.M. Ravi, P. Will, J. Kueckelhaus, N. Sun, K. Joseph, H. Salié, L. Vollmer, U. Kuliesiute, J. von Ehr, J.K. Benotmane, N. Neidert, M. Follo, F. Scherer, J. M. Goeldner, S.P. Behringer, P. Franco, M. Khiat, J. Zhang, U.G. Hofmann, C. Fung, F.L. Ricklefs, K. Lamszus, M. Boerries, M. Ku, J. Beck, R. Sankowski, M. Schwabenland, M. Prinz, U. Schüller, S. Killmer, B. Bengsch, A.K. Walch, D. Delev, O. Schnell, D.H. Heiland, Spatially resolved multi-omics deciphers bidirectional tumor-host interdependence in glioblastoma, Cancer Cell 40 (2022) 639–655.e13.

[48] T. Shekarian, C.P. Zinner, E.M. Bartoszek, W. Duchemin, A.T. Wachnowicz, S. Hogan, M.M. Etter, J. Flammer, C. Paganetti, T.A. Martins, P. Schmassmann, S. Zanganeh, F. Le Goff, M.G. Muraro, M.-F. Ritz, D. Phillips, S.S. Bhate, G. L. Barlow, G.P. Nolan, C.M. Schürch, G. Hutter, Immunotherapy of glioblastoma explants induces interferon-γ responses and spatial immune cell rearrangements in tumor center, but not periphery, Sci. Adv. 8 (2022), https://doi.org/10.1126/sciadv.abn9440.

[49] Y. Zheng, F. Carrillo-Perez, M. Pizurica, D.H. Heiland, O. Gevaert, Spatial cellular architecture predicts prognosis in glioblastoma, Nat. Commun. 14 (2023), https://doi.org/10.1038/s41467-023-39933-0.

[50] W. Ren, W. Fu, X. Wu, J. Chen, Towards the ground state of molecules via diffusion Monte Carlo on neural networks, Nat. Commun. 14 (2023), https://doi.org/10.1038/s41467-023-37609-3.

[51] A.C. Greenwald, N.G. Darnell, R. Hoefflin, D. Simkin, C.W. Mount, L.N. Gonzalez Castro, Y. Harnik, S. Dumont, D. Hirsch, M. Nomura, T. Talpir, M. Kedmi, I. Goliand, G. Medici, J. Laffy, B. Li, V. Mangena, H. Keren-Shaul, M. Weller, Y. Addadi, M.C. Neidert, M.L. Suvà, I. Tirosh, Integrative spatial analysis reveals a multi-layered organization of glioblastoma, Cell 187 (2024) 2485–2501.e26.

[52] A.L. Johnson, H. Lopez-Bertoni, Cellular diversity through space and time: adding new dimensions to GBM therapeutic development, Front. Genet. 15 (2024) 1356611.

[53] Y.A. Yabo, P.M. Moreno-Sanchez, Y. Pires-Afonso, T. Kaoma, B. Nosirov, A. Scafidi, L. Ermini, A. Lipsa, A. Oudin, D. Kyriakis, K. Grzyb, S.K. Poovathingal, A. Poli, A. Muller, R. Toth, B. Klink, G. Berchem, C. Berthold, F. Hertel, M. Mittelbronn, D. H. Heiland, A. Skupin, P.V. Nazarov, S.P. Niclou, A. Michelucci, A. Golebiewska, Glioblastoma-instructed microglia transition to heterogeneous phenotypic states with phagocytic and dendritic cell-like features in patient tumors and patient-derived orthotopic xenografts, Genome Med 16 (2024), https://doi.org/10.1186/s13073-024-01321-8.

[54] D. Yuan, W. Chen, S. Jin, W. Li, W. Liu, L. Liu, Y. Wu, Y. Zhang, X. He, J. Jiang, H. Sun, X. Liu, J. Liu, Co-expression of immune checkpoints in glioblastoma revealed by single-nucleus RNA sequencing and spatial transcriptomics, Comput. Struct. Biotechnol. J. 23 (2024) 1534–1546.

[55] M. Motevasseli, M. Darvishi, A. Khoshnevisan, M. Zeinalizadeh, H. Saffar, S. Bayat, A. Najafi, M.J. Abbaspour, A. Mamivand, S.B. Olson, M. Tabrizi, Distinct tumor-TAM interactions in IDH-stratified glioma microenvironments unveiled by single-cell and spatial transcriptomics, BioRxiv (2024). ⟨https://doi.org/10.1186/s40478-024-01837-5⟩.

[56] K.-S. Kim, J. Zhang, V.A. Arrieta, C. Dmello, E. Grabis, K. Habashy, J. Duffy, J. Zhao, A. Gould, L. Chen, J. Hu, I. Balyasnikova, D. Chand, D. Levey, P. Canoll, W. Zhao, P.A. Sims, R. Rabadan, S. Pandey, B. Zhang, C. Lee-Chang, D.H. Heiland, A.M. Sonabend, MAPK/ERK signaling in gliomas modulates interferon responses, T cell recruitment, microglia phenotype, and immune checkpoint blockade efficacy, BioRxivorg (2024), https://doi.org/10.1101/2024.09.11.612571.

[57] D.H. Heiland, A. Gaebelein, M. Börries, J. Wörner, N. Pompe, P. Franco, S. Heynckes, M. Bartholomae, D.Ó. hAilín, M.S. Carro, M. Prinz, S. Weber, I. Mader, D. Delev, O. Schnell, Microenvironment-derived regulation of HIF signaling drives transcriptional heterogeneity in glioblastoma multiforme, Mol. Cancer Res. 16 (2018) 655–668.

[58] L. Wu, W. Wu, J. Zhang, Z. Zhao, L. Li, M. Zhu, M. Wu, F. Wu, F. Zhou, Y. Du, R.-C. Chai, W. Zhang, X. Qiu, Q. Liu, Z. Wang, J. Li, K. Li, A. Chen, Y. Jiang, X. Xiao, H. Zou, R. Srivastava, T. Zhang, Y. Cai, Y. Liang, B. Huang, R. Zhang, F. Lin, L. Hu, X. Wang, X. Qian, S. Lv, B. Hu, S. Zheng, Z. Hu, H. Shen, Y. You, R.G.W. Verhaak, T. Jiang, Q. Wang, Natural coevolution of tumor and immunoenvironment in glioblastoma, Cancer Discov. 12 (2022) 2820–2837.

[59] R.L. Jensen, M.L. Mumert, D.L. Gillespie, A.Y. Kinney, M.C. Schabel, K.L. Salzman, Preoperative dynamic contrast-enhanced MRI correlates with molecular markers of hypoxia and vascularity in specific areas of intratumoral microenvironment and is predictive of patient outcome, Neuro. Oncol. 16 (2014) 280–291.

[60] S. Coy, S. Wang, S.A. Stopka, J.-R. Lin, C. Yapp, C.C. Ritch, L. Salhi, G.J. Baker, R. Rashid, G. Baquer, M. Regan, P. Khadka, K.A. Cole, J. Hwang, P.Y. Wen, P. Bandopadhayay, M. Santi, T. De Raedt, K.L. Ligon, N.Y.R. Agar, P.K. Sorger, M. Touat, S. Santagata, Single cell spatial analysis reveals the topology of immunomodulatory purinergic signaling in glioblastoma, Nat. Commun. 13 (2022), https://doi.org/10.1038/s41467-022-32430-w.

[61] M.J. Haley, L. Bere, J. Minshull, S. Georgaka, N. Garcia-Martin, G. Howell, D. J. Coope, F. Roncaroli, A. King, D.C. Wedge, S.M. Allan, O.N. Pathmanaban, D. Brough, K.N. Couper, Hypoxia coordinates the spatial landscape of myeloid cells within glioblastoma to affect survival, Sci. Adv. 10 (2024), https://doi.org/10.1126/sciadv.adj3301.

[62] A. Rashidi, L.K. Billingham, A. Zolp, T.-Y. Chia, C. Silvers, J.L. Katz, C.H. Park, S. Delay, L. Boland, Y. Geng, S.M. Markwell, C. Dmello, V.A. Arrieta, K. Zilinger, I. M. Jacob, A. Lopez-Rosas, D. Hou, B. Castro, A.M. Steffens, K. McCortney, J. P. Walshon, M.S. Flowers, H. Lin, H. Wang, J. Zhao, A. Sonabend, P. Zhang, A. U. Ahmed, D.J. Brat, D.H. Heiland, C. Lee-Chang, M.S. Lesniak, N.S. Chandel, J. Miska, Myeloid cell-derived creatine in the hypoxic niche promotes glioblastoma growth, Cell Metab. 36 (2024) 62–77.e8.

[63] D.J. Kloosterman, J. Erbani, M. Boon, M. Farber, S.M. Handgraaf, M. Ando-Kuri, E. Sánchez-López, B. Fontein, M. Mertz, M. Nieuwland, N.Q. Liu, G. Forn-Cuni, N. N. van der Wel, A.E. Grootemaat, L. Reinalda, S.I. van Kasteren, E. de Wit, B. Ruffell, E. Snaar-Jagalska, K. Petrecca, D. Brandsma, A. Kros, M. Giera, L. Akkari, Macrophage-mediated myelin recycling fuels brain cancer malignancy, Cell 187 (2024) 5336–5356.e30.

[64] A. Mossi Albiach, J. Janusauskas, I. Kapustová, E. Kvedaraite, S. Codeluppi, J. B. Munting, L.E. Borm, J. Kjaer Jacobsen, A. Shamikh, O. Persson, S. Linnarsson, Glioblastoma is spatially organized by neurodevelopmental programs and a glial-like wound healing response, BioRxiv (2023), https://doi.org/10.1101/2023.09.01.555882.

[65] C. Calabrese, H. Poppleton, M. Kocak, T.L. Hogg, C. Fuller, B. Hamner, E.Y. Oh, M. W. Gaber, D. Finklestein, M. Allen, A. Frank, I.T. Bayazitov, S.S. Zakharenko, A. Gajjar, A. Davidoff, R.J. Gilbertson, A perivascular niche for brain tumor stem cells, Cancer Cell 11 (2007) 69–82.

[66] D.A. Aderetti, V.V.V. Hira, R.J. Molenaar, C.J.F. van Noorden, The hypoxic peri-arteriolar glioma stem cell niche, an integrated concept of five types of niches in human glioblastoma, Biochim. Biophys. Acta Rev. Cancer 1869 (2018) 346–354.

[67] Y. Liu, Z. Wu, Y. Feng, J. Gao, B. Wang, C. Lian, B. Diao, Integration analysis of single-cell and spatial transcriptomics reveal the cellular heterogeneity landscape in glioblastoma and establish a polygenic risk model, Front. Oncol. 13 (2023), https://doi.org/10.3389/fonc.2023.1109037.

[68] E. Karimi, M.W. Yu, S.M. Maritan, L.J.M. Perus, M. Rezanejad, M. Sorin, M. Dankner, P. Fallah, S. Doré, D. Zuo, B. Fiset, D.J. Kloosterman, L. Ramsay, Y. Wei, S. Lam, R. Alsajjan, I.R. Watson, G. Roldan Urgoiti, M. Park, D. Brandsma, D.L. Senger, J.A. Chan, L. Akkari, K. Petrecca, M.-C. Guiot, P.M. Siegel, D.F. Quail, L.A. Walsh, Single-cell spatial immune landscapes of primary and metastatic brain tumours, Nature 614 (2023) 555–563.

[69] A.Z. Wang, B.L. Mashimo, M.O. Schaettler, N.D. Sherpa, L.A. Leavitt, A. J. Livingstone, S.M. Khan, M. Li, M.I. Anzaldua-Campos, J.D. Bradley, E. C. Leuthardt, A.H. Kim, J.L. Dowling, M.R. Chicoine, P.S. Jones, B.D. Choi, D. P. Cahill, B.S. Carter, A.A. Petti, T.M. Johanns, G.P. Dunn, Glioblastoma-infiltrating CD8+ T cells are predominantly a clonally expanded GZMK+ effector population, Cancer Discov. 14 (2024) 1106–1131.

[70] M. Liu, Z. Ji, V. Jain, V.L. Smith, E. Hocke, A.P. Patel, R.E. McLendon, D.M. Ashley, S.G. Gregory, G.Y. López, Spatial transcriptomics reveals segregation of tumor cell states in glioblastoma and marked immunosuppression within the perinecrotic niche, Acta Neuropathol. Commun. 12 (2024), https://doi.org/10.1186/s40478-024-01769-0.

[71] C. Ruiz-Moreno, S.M. Salas, E. Samuelsson, S. Brandner, M.E.G. Kranendonk, M. Nilsson, H.G. Stunnenberg, Harmonized single-cell landscape, intercellular crosstalk and tumor architecture of glioblastoma, BioRxiv (2022), https://doi.org/10.1101/2022.08.27.505439.

[72] K.R. Taylor, T. Barron, A. Hui, A. Spitzer, B. Yalçin, A.E. Ivec, A.C. Geraghty, G. G. Hartmann, M. Arzt, S.M. Gillespie, Y.S. Kim, S. Maleki Jahan, H. Zhang, K. Shamardani, M. Su, L. Ni, P.P. Du, P.J. Woo, A. Silva-Torres, H.S. Venkatesh, R. Mancusi, A. Ponnuswami, S. Mulinyawe, M.B. Keough, I. Chau, R. Aziz-Bose, I. Tirosh, M.L. Suvà, M. Monje, Glioma synapses recruit mechanisms of adaptive plasticity, Nature 623 (2023) 366–374.

[73] H.S. Venkatesh, T.B. Johung, V. Caretti, A. Noll, Y. Tang, S. Nagaraja, E.M. Gibson, C.W. Mount, J. Polepalli, S.S. Mitra, P.J. Woo, R.C. Malenka, H. Vogel, M. Bredel, P. Mallick, M. Monje, Neuronal activity promotes glioma growth through neuroligin-3 secretion, Cell 161 (2015) 803–816.

[74] D.S.L. Harwood, V. Pedersen, N.S. Bager, A.Y. Schmidt, T.O. Stannius, A. Areškevičiūtė, K. Josefsen, D.S. Nørøxe, D. Scheie, H. Rostalski, M.J.S. Lü, A. Locallo, U. Lassen, F.O. Bagger, J. Weischenfeldt, D.H. Heiland, K. Vitting-Seerup, S.R. Michaelsen, B.W. Kristensen, Glioblastoma cells increase expression of notch signaling and synaptic genes within infiltrated brain tissue, Nat. Commun. 15 (2024) 7857.

[75] S.L. Campbell, S.C. Buckingham, H. Sontheimer, Human glioma cells induce hyperexcitability in cortical networks, Epilepsia 53 (2012) 1360–1370.

[76] R. Drexler, R. Khatri, T. Sauvigny, M. Mohme, C.L. Maire, A. Ryba, Y. Zghaibeh, L. Dührsen, A. Salviano-Silva, K. Lamszus, M. Westphal, J. Gempt, A.K. Wefers, J. E. Neumann, H. Bode, F. Hausmann, T.B. Huber, S. Bonn, K. Jütten, D. Delev, K. J. Weber, P.N. Harter, J. Onken, P. Vajkoczy, D. Capper, B. Wiestler, M. Weller, B. Snijder, A. Buck, T. Weiss, P.C. Göller, F. Sahm, J.A. Menstel, D.N. Zimmer, M. B. Keough, L. Ni, M. Monje, D. Silverbush, V. Hovestadt, M.L. Suvà, S. Krishna, S. L. Hervey-Jumper, U. Schüller, D.H. Heiland, S. Hänzelmann, F.L. Ricklefs,

A prognostic neural epigenetic signature in high-grade glioma, Nat. Med. (2024), https://doi.org/10.1038/s41591-024-02969-w.
[77] K. Tanaka, H. Waki, Y. Ido, S. Akita, Y. Yoshida, T. Yoshida, T. Matsuo, Protein and polymer analyses up to m/z 100 000 by laser ionization time-of-flight mass spectrometry, Rapid Commun. Mass Spectrom. 2 (1988) 151–153.
[78] M. Karas, D. Bachmann, U. Bahr, F. Hillenkamp, Matrix-assisted ultraviolet laser desorption of non-volatile compounds, Int. J. Mass Spectrom. Ion.-. Process. 78 (1987) 53–68.
[79] T. Lu, L. Freytag, V.K. Narayana, Z. Moore, S.J. Oliver, A. Valkovic, B. Nijagal, A. L. Peterson, D.P. de Souza, M.J. McConville, J.R. Whittle, S.A. Best, S. Freytag, Matrix selection for the visualization of small molecules and lipids in brain tumors using untargeted MALDI-TOF mass spectrometry imaging, Metabolites 13 (2023) 1139.
[80] L. Gao, G. Li, J. Cyriac, Z. Nie, R.G. Cooks, Imaging of surface charge and the mechanism of desorption electrospray ionization mass spectrometry, J. Phys. Chem. C. Nanomater. Interfaces 114 (2010) 5331–5337.
[81] L.A. Lyon, C.D. Keating, A.P. Fox, B.E. Baker, L. He, S.R. Nicewarner, S. P. Mulvaney, M.J. Natan, Raman spectroscopy, Anal. Chem. 70 (1998) 341R–361R.
[82] P. Kukura, D.W. McCamant, R.A. Mathies, Femtosecond stimulated Raman spectroscopy, Annu. Rev. Phys. Chem. 58 (2007) 461–488.
[83] K.E. Kay, J. Lee, E.S. Hong, J. Beilis, S. Dayal, E. Wesley, S. Mitchell, S.Z. Wang, D. J. Silver, J. Volovetz, S. Johnson, M. McGraw, M.M. Grabowski, T. Lu, L. Freytag, V. Narayana, S. Freytag, S.A. Best, J.R. Whittle, Z. Wang, O. Reizes, J.S. Yu, S. L. Hazen, J.M. Brown, D. Bayik, J.D. Lathia, Tumor cell-derived spermidine promotes a pro-tumorigenic immune microenvironment in glioblastoma via CD8+ T cell inhibition, BioRxiv (2023), https://doi.org/10.1172/JCI177824.
[84] J. Miska, A. Rashidi, C. Lee-Chang, P. Gao, A. Lopez-Rosas, P. Zhang, R. Burga, B. Castro, T. Xiao, Y. Han, D. Hou, S. Sampat, A. Cordero, J.S. Stoolman, C. M. Horbinski, M. Burns, Y.K. Reshetnyak, N.S. Chandel, M.S. Lesniak, Polyamines drive myeloid cell survival by buffering intracellular pH to promote immunosuppression in glioblastoma, Sci. Adv. 7 (2021), https://doi.org/10.1126/sciadv.abc8929.
[85] L.S. Eberlin, I. Norton, A.L. Dill, A.J. Golby, K.L. Ligon, S. Santagata, R.G. Cooks, N. Y.R. Agar, Classifying human brain tumors by lipid imaging with mass spectrometry, Cancer Res. 72 (2012) 645–654.
[86] E.C. Randall, B.G.C. Lopez, S. Peng, M.S. Regan, W.M. Abdelmoula, S.S. Basu, S. Santagata, H. Yoon, M.C. Haigis, J.N. Agar, N.L. Tran, W.F. Elmquist, F. M. White, J.N. Sarkaria, N.Y.R. Agar, Localized metabolomic gradients in patient-derived xenograft models of Glioblastoma, Cancer Res. 80 (2020) 1258–1267.
[87] A. Baig Mirza, I. Christodoulides, J.P. Lavrador, A. Giamouriadis, A. Vastani, T. Boardman, R. Ahmed, I. Norman, C. Murphy, S. Devi, F. Vergani, R. Gullan, R. Bhangoo, K. Ashkan, 5-Aminolevulinic acid-guided resection improves the overall survival of patients with glioblastoma—a comparative cohort study of 343 patients, Neuro Oncol. Adv. 3 (2021) vdab047.
[88] J.L. Ross, L.A.D. Cooper, J. Kong, D. Gutman, M. Williams, C. Tucker-Burden, M. R. McCrary, A. Bouras, M. Kaluzova, W.D. Dunn, Jr, D. Duong, C.G. Hadjipanayis, D.J. Brat, 5-aminolevulinic acid guided sampling of glioblastoma microenvironments identifies pro-survival signaling at infiltrative margins, Sci. Rep. 7 (2017), https://doi.org/10.1038/s41598-017-15849-w.
[89] G. Andrieux, T. Das, M. Griffin, J. Straehle, S.M.L. Paine, J. Beck, M. Boerries, D. H. Heiland, S.J. Smith, R. Rahman, S. Chakraborty, Spatially resolved transcriptomic profiles reveal unique defining molecular features of infiltrative 5ALA-metabolizing cells associated with glioblastoma recurrence, Genome Med 15 (2023), https://doi.org/10.1186/s13073-023-01207-1.
[90] V. Bhandari, C. Hoey, L.Y. Liu, E. Lalonde, J. Ray, J. Livingstone, R. Lesurf, Y.-J. Shiah, T. Vujcic, X. Huang, S.M.G. Espiritu, L.E. Heisler, F. Yousif, V. Huang, T. N. Yamaguchi, C.Q. Yao, V.Y. Sabelnykova, M. Fraser, M.L.K. Chua, T. van der Kwast, S.K. Liu, P.C. Boutros, R.G. Bristow, Molecular landmarks of tumor hypoxia across cancer types, Nat. Genet. 51 (2019) 308–318.
[91] K. Synnestvedt, G.T. Furuta, K.M. Comerford, N. Louis, J. Karhausen, H. K. Eltzschig, K.R. Hansen, L.F. Thompson, S.P. Colgan, Ecto-5′-nucleotidase (CD73) regulation by hypoxia-inducible factor-1 mediates permeability changes in intestinal epithelia, J. Clin. Invest. 110 (2002) 993–1002.
[92] T.P. Plesec, R.A. Prayson, Frozen section discrepancy in the evaluation of central nervous system tumors, Arch. Pathol. Lab. Med. 131 (2007) 1532–1540.
[93] H.L. Somerset, B.K. Kleinschmidt-DeMasters, Approach to the intraoperative consultation for neurosurgical specimens, Adv. Anat. Pathol. 18 (2011) 446–449.
[94] J. Herta, A. Cho, T. Roetzer-Pejrimovsky, R. Höftberger, W. Marik, G. Kronreif, T. Peilnsteiner, K. Rössler, S. Wolfsberger, Optimizing maximum resection of glioblastoma: Raman spectroscopy versus 5-aminolevulinic acid, J. Neurosurg. 139 (2023) 334–343.
[95] M.L. Calabretto, L. Giol, S. Sulfaro, Diagnostic utility of cell-block from bronchial washing in pulmonary neoplasms, Diagn. Cytopathol. 15 (1996) 191–192.
[96] S. Santagata, L.S. Eberlin, I. Norton, D. Calligaris, D.R. Feldman, J.L. Ide, X. Liu, J. S. Wiley, M.L. Vestal, S.H. Ramkissoon, D.A. Orringer, K.K. Gill, I.F. Dunn, D. Dias-Santagata, K.L. Ligon, F.A. Jolesz, A.J. Golby, R.G. Cooks, N.Y.R. Agar, Intraoperative mass spectrometry mapping of an onco-metabolite to guide brain tumor surgery, Proc. Natl. Acad. Sci. 111 (2014) 11121–11126.
[97] K.M. Hotchkiss, P. Karschnia, K.C. Schreck, M. Geurts, T.F. Cloughesy, J. Huse, E. S. Duke, J. Lathia, D.M. Ashley, E.K. Nduom, G. Long, K. Singh, A. Chalmers, M. S. Ahluwalia, A. Heimberger, S. Bagley, T. Todo, R. Verhaak, P.D. Kelly, S. Hervey-Jumper, J. de Groot, A. Patel, P. Fecci, I. Parney, V. Wykes, C. Watts, T.C. Burns, N. Sanai, M. Preusser, J.C. Tonn, K.J. Drummond, M. Platten, S. Das, K. Tanner, M. A. Vogelbaum, M. Weller, J.R. Whittle, M.S. Berger, M. Khasraw, A brave new framework for glioma drug development, Lancet Oncol. 25 (2024) e512–e519.